Published in final edited form as:
Nanotoxicology. 2014 December ; 8(8): 856–866. doi:10.3109/17435390.2013.837208.

Low-Dose gold nanoparticles exert subtle endocrine-modulating effects on the ovarian steroidogenic pathway *ex vivo* independent of oxidative stress

Jeremy K Larson, **Michael J Carvan III**, **Justin G Teeguarden**, **Gen Watanabe**, **Kazuyoshi Taya**, **Evan Krystofiak**, and **Reinhold J Hutz**

Abstract

Gold nanoparticles (GNPs) have gained considerable attention for application in science and industry. However, the untoward effects of such particles on female fertility remain unclear. The objectives of the present study were to (1) examine the effects of 10-nm GNPs on progesterone and estradiol-17β accumulation by rat ovaries *ex vivo* and (2) to identify the locus/loci whereby GNPs modulate steroidogenesis via multiple-reference gene quantitative real-time RT-PCR. Regression analyses indicated a positive relationship between both *Star* ($p<0.05$, $r^2= 0.278$) and *Cyp11a1* ($p<0.001$, $r^2= 0.366$) expression and P4 accumulation upon exposure to 1.43×10^6 GNPs/mL. Additional analyses showed that E2 accumulation was positively associated with *Hsd3b1* ($p<0.05$, $r^2= 0.181$) and *Cyp17a1* ($p<0.01$, $r^2= 0.301$) expression upon exposure to 1.43×10^3 and 1.43×10^9 GNPs/mL, respectively. These results suggest a subtle treatment-dependent impact of low-dose GNPs on the relationship between progesterone or estradiol-17β and specific steroidogenic target genes, independent of oxidative stress or inhibin.

INTRODUCTION

Gold nanoparticles (GNPs) have gained considerable attention for potential novel applications in industry (Ngo et al. 2011), consumer products (Sung et al. 2011), and medicine (Libutti et al. 2010). However, despite these advances toward potential therapeutic and current consumer benefit of GNPs, concern has arisen as to the possible toxicologic consequences of such molecules within biologic systems and the environment. For instance, it has been shown that *in-vivo* exposure to GNPs can induce pulmoand neurotoxicity

DECLARATION OF INTEREST

The authors have no competing financial interests.

(Hussain et al. 2011; Chen et al. 2010). Research has also shown that GNPs can alter gene expression (Truong et al. 2012); initiate oxidative stress-mediated cell death (Gao et al. 2011); and modulate cellular function (Li et al. 2011). Moreover, potential human exposure to such particles is likely to be widespread as nanogold is the sixth most common nanoparticle type exploited for consumer benefit (*i.e.,* 28 of 1,317 known nanotechnology-based consumer products list GNPs as a component) as reported by the Project on Emerging Nanotechnologies (Woodrow Wilson International Center for Scholars, 2012; Kessler 2011). In tandem, the wide distribution of GNPs and likely increases in future uses highlight the potential risk for environmental and occupational exposures to GNPs that might ultimately cause detrimental health effects to workers and the general population.

Recent work from our laboratory has shown that 10-nm GNPs can enter rat granulosa cells, translocate into lipid droplets, alter mitochondrial morphology, and subsequently modulate estradiol-17β (E2) accumulation *in vitro* (Stelzer and Hutz 2009). Transmission electron microscopic (TEM) studies showed that 10-nm GNPs were found inside apparently damaged and swollen mitochondria. This evidence suggests to us that GNPs may be capable of disrupting ovarian steroidogenesis via oxidative stress—an established outcome of mitochondrial damage (Cai et al. 1998) and inhibitor of steroidogenesis (Diemer et al. 2003)—that may ultimately lead to reduced female reproductive function and fertility.

Other recent studies have shown that engineered nanoparticles can enter the rodent ovary *in vivo*. For instance, Arnida et al. (2011) have demonstrated the entry of PEGlygated 50-nm GNPs into an orthotopic ovarian tumor in a mouse model. Gao et al. (2012) have also suggested that titanium oxide (TiO_2) nanoparticles (~6 nm; 10 mg/kg body weight) accumulated in mouse ovary after 90 consecutive days of intragastric administration; and subsequently damaged mitochondria, which in turn induced oxidative stress and apoptosis *in vivo*. DNA microarray results indicated significant upregulation of genes associated with sex-steroid synthesis and reproduction (e.g., *Star*, *Cyplla1*, and *Cyp17a1*), apoptosis (e.g., *BCl2a1b*) and oxidative stress (e.g., *Gpx3*). Importantly, serum concentrations of E2 and progesterone (P4) in TiO2 nanoparticle-exposed mice were significantly elevated compared to controls ($p<0.05$). However, Wang et al. (2011) demonstrated that exposure of adult zebrafish to TiO2 nanoparticles (240–280 nm) for 13 weeks resulted in a significant reduction in the expression of *Cyp11a1*. In contrast, *in-vivo* exposure of female rats to zinc oxide (ZnO) nanoparticles (20–30 nm) for 5 days after administration via oral gavage had no effect on the serum concentration of E2 compared to controls ($p>0.05$) (Esmaeillou et al. 2013). Similarly, calcium phosphate ($Ca_3[PO4]_2$) nanoparticles had no effect on E2 or P4 accumulation or on *Star*, *Cyp17a1*, or *Cyp19a1* expression in a luteinized human granulosa cell model (Lui et al. 2010). Collectively, the evidence suggests that the ovarian steroidogenic pathway may be an important target of nanotoxicity that requires further investigation. We hypothesized that *ex-vivo* exposure of intact rat ovary to GNPs will perturb E2, P4, and inhibin secretion/accumulation in culture and ultimately diminish their production long-term via an oxidative stress-mediated mechanism. We postulated that GNPs accumulate in the ovaries of humans or animals as a result of unintended occupational and/or environmental exposure(s) to GNPs and potentially exert endocrine-disrupting effects that may ultimately impact female fertility.

Therefore, the objectives of the present study were to (1) evaluate potential time- and dose-dependent effects of GNPs on *ex-vivo* accumulation of ovarian E2, progesterone (P4), and inhibin and; and (2) to evaluate the locus (loci) of endocrine disruption in rat ovarian steroidogenesis by GNPs using multiple reference gene-quantitative real-time RT-PCR to target expression of steroidogenesis (*Star*, *Cyp11a1*, *Cyp17a1*, *Hsd3b1*, and *Cyp19a1*)- and oxidative stress (*Hmox1* and *Sod2*)-related genes.

MATERIALS AND METHODS

Materials and methods are summarized below. More detail is included as Supplemental Material.

Materials

Gold nanoparticles (GNPs; 10 nm, 5.70×10^{12} particles/mL) synthesized by citrate reduction and dispersed in double-distilled water were purchased from Nanocs, Inc. (New York, NY, USA). The following supplies and reagents were purchased: 1-mL center-well culture dishes from Becton Dickinson and Co. (Franklin Lakes, NJ, USA), equine chorionic gonadotropin (eCG) and follicle-stimulating hormone (FSH) from EMD Biosciences Inc. (La Jolla, CA, USA), DMEM/F-12 50/50 medium without phenol red and with L-glutamine from Mediatech Inc. (Manassas, VA, USA), fetal calf serum (FCS) and and rostenedione (A4) from Sigma-Aldrich (St. Louis, MO, USA), gentamicin reagent solution (10mg/mL) from MP Biomedicals LLC (Solon, OH, USA), Trizol® from Invitrogen Corporation (Carlsbad, CA, USA), E2 and P4 radioimmunoassay kits from Siemens's Medical Solutions Diagnostics (Los Angeles, CA, USA), RQ1 RNAse-Free DNAse from Promega Corporation (Madison, WI, USA), AffinityScript® Multiple Temperature cDNA Synthesis Kit from Agilent Technologies (La Jolla, CA, USA), *Power* SYBR® Green PCR Master Mix from Life Technologies Corp. (Carlsbad, CA, USA), and gene-specific primers from Integrated DNA Technologies, Inc. (Coralville, IA, USA).

Animals

The IACUC at the University of Wisconsin-Milwaukee approved all experimental protocols. Animals were housed two to a cage in a room with constant temperature (22 ± 2°C), humidity (55 ± 5%) and light cycle (12L: 12D; lights on 07:00). Pre-pubertal female rats (n= 120), Sprague-Dawley, *Rattus norvegicus*; age= 21 days old; Charles River Laboratories, Wilmington, MA, USA) were injected with 10 IU/ml equine chorionic gonadotropin (eCG) to stimulate ovarian follicular development. Animals were sacrificed 72 hours post injection by carbon dioxide asphyxiation and ovaries were removed. Animal trial refers to each individual cohort of rats purchased and is equivalent to one experiment. Four separate experiments were conducted and each experiment entailed 30 rats.

Electron Microscopy

Transmission electron microscopy (TEM) imaging using a Hitachi H-600 microscope (Pleasanton, CA, USA) was performed to characterize both stock and experimental GNPs (Stelzer and Hutz 2009). Hereafter, the term "stock GNPs" refers to the GNPs dispersed in double-distilled water that were received from Nanocs, Inc, and "experimental GNPs" refers

to stock GNPs that were suspended in culture medium (1.43×10^3, 1.43×10^6, or 1.43×10^9 particles/mL) and exposed to experimental conditions (see Ex-Vivo *Culture of Rat Ovary* below). High-resolution TEM (HRTEM) and scanning electron microscopy (SEM) were conducted using a Hitachi H-9500 300 kV microscope and a Hitachi S-4800 microscope, respectively (Pleasanton, CA, USA). Both approaches were solely used to characterize our stock GNPs. Particle size and distribution were determined using *Image J* analysis software (NIH, Bethesda, MD, USA).

Dynamic Light-Scattering Spectroscopy (DLS)

A Malvern Zeta-sizer Nano Zs (Malvern Instruments, Southborough, MA, USA) was employed to analyze the zeta potential and hydrodynamic diameter of both our stock and experimental GNPs (1.43×10^3, 1.43×10^6, or 1.43×10^9 particles/mL). DLS analyses of our stock and experimental GNPs were conducted using similar procedures.

X-ray Photoelectron Spectroscopy (XPS)

XPS was utilized to characterize the surface chemistry of our stock GNPs. Measurements were performed using a Kratos Axis Ultra DLD spectrometer with a monochromatic Al Kα X-ray (1486.7 eV) source at 10 mA, 15 kV for excitation.

Pyrogene™ Recombinant Factor C (rFC) Endotoxin Detection Assay

rFC assays were conducted by Lonza, Inc. (SOP 162.19; Walkersville, MD, USA) to evaluate the concentration of endotoxin present in non-incubated samples of our GNP-supplemented culture solutions as a function of experimental GNP concentration.

Ex-vivo Culture of Rat Ovary

After surgical removal, ovaries (n= 240) were bathed in 3 ml of culture medium supplemented with 50 μg/mL gentamicin, and carefully trimmed of excess tissue. Ovaries from each rat remained paired; thus, one ovary was cultured under control conditions and the other under treatment conditions (1.43×10^3, 1.43×10^6, or 1.43×10^9 particles/mL medium) (Figure 1). Assuming that a 15-nm GNP contains 37,000 gold atoms (Harper et al., 2011), the mass concentrations of each *ex-vivo* dose of GNPs (*i.e.*, 1.59 fg gold/mL, 1.59 pg gold/mL, and 1.59 ng gold/mL) and the stock GNP solution (*i.e.*, 6.42 μg gold/mL) were mathematically calculated using a mean primary diameter (MPD) of 6.77 nm. This MPD was chosen based on the TEM results for our stock GNPs. The mass concentration of the purchased stock GNPs was not provided by the manufacturer. MEM/F12 50/50 medium was supplemented with 5% fetal calf serum (FCS) 50 μg/mL gentamicin, 50 ng/mL follicle-stimulating hormone (FSH) and 1×10^{-7} M androstenedione (A4) to ensure adequate stimulation of ovarian steroidogenesis. GNPs were vortexed but not sonicated prior to suspension in the culture medium. Upon suspension, each solution was vortexed before each 1-mL aliquot was removed, and placed in a 1-mL center-well culture dish. Ovaries were then gently placed on a small piece of nylon mesh (1.25 cm × 1.25 cm) overlaying the culture medium in each culture dish (either control or treatment condition) and incubated at 37°C in 5% CO_2 in air for 12, 24, or 48 hours. Each ovary was then transferred to a 1.5-mL centrifuge tube containing 500 μl Trizol® and immediately snap-frozen on dry ice and

stored at −80°C until ready for RNA extraction. Each 1-mL aliquot of culture medium was transferred to a 1.5-ml centrifuge tube, snap-frozen, and stored at −80°C for radioimmunoassay.

Use of the *In-vitro* Sedimentation, Diffusion, and Dosimetry Model (ISDD) to Estimate Target-Tissue Dose

ISDD (Hinderliter et al. 2010) was employed to estimate the GNP *ex-vivo* target-tissue dose (*i.e.*, dose of GNPs delivered to each treated ovary in our *ex-vivo* model) because the gold content of the ovarian tissue was below the limits of detection by standard analytical techniques (*e.g.*, we initially used inductively coupled plasma-mass spectrometry). ISDD theoretically estimates the target-cell dose of nanoparticles in a monolayer-cell-culture system using the following characteristics of an *in-vitro* model: medium height, medium density, medium viscosity, particle density, temperature, and hydrodynamic particle diameter. We adapted this model to our *ex-vivo* tissue-culture paradigm using the MPD of our experimental GNPs (10 nm) derived from TEM rather than the mean hydrodynamic diameter (MHD) since DLS was insufficient for evaluating the MHD of our experimental GNPs due to the inclusion of extremely low particle concentrations in our study.

Radioimmunoassay

Radioimmunoassay (RIA) of P4/E2 and inhibin was conducted according to Stelzer and Hutz (2009) and Ho et al. (2006), respectively (Figure 1). The average intra-assay coefficients of variation (CV) for our E2 and P4 RIAs were 6.92% and 7.30%, respectively. The intra- and inter-assay CVs for our inhibin RIAs were 4.0% and 6.2%, respectively. The measured concentrations of E2, P4, and inhibin by RIA were normalized to total ovarian RNA to account for differences in ovarian size/weight (Trkulja and Lackovic et al. 2001). Control hormone values were normalized to 1.0 and treatments were then compared to each paired control.

Multiple-Reference Gene-quantitative Real-Time RT-PCR (MRG-qPCR)

Following homogenization, an additional 500 μl Trizol® was added to each thawed ovary/Trizol sample. RNA from each sample was isolated per the manufacturer's protocol for Trizol®. RNA was purified via ethanol precipitation. RNA quality was analyzed using agarose gel electrophoresis and spectrophotometry (Nanodrop ND-1000, Wilmington, DE, USA). RNA samples (1 μg) were then treated with RQ1 RNAse-Free DNAse prior to cDNA synthesis using the AffinityScript® Multiple Temperature cDNA Synthesis Kit per manufacturer's protocol. Expression stability of our reference genes for rat ovary (*i.e.*, *Gapdh, Actb, and Zc3h1*) was extensively validated via evaluation of the cycle threshold (C_t) variance under our experimental conditions prior to MRG-qPCR. The quantity of each target gene, normalized to the geometric mean of our chosen reference genes (Vandesompele et al., 2002) and relative to a reference control sample, was calculated by $2^{-\Delta\Delta C_T}$ (Pfaffl 2001) using StepOne™ Software (version 2.1) (Figure 1). The inter-assay and intra-assay CV for all conducted qPCR assays were 1.76% and 0.62%, respectively.

Statistics—All RIA and qPCR data were spline- or $\log_2$- transformed, respectively. Two-way ANOVA was used to evaluate the *dramatic end-point effects* of incubation period and

GNP concentration on hormone accumulation in culture. Regression models are sensitive in their detection of the underlying nonmonotonic biologic responses often observed with low-dose endocrine-disrupting compounds in comparison to the more omnibus ANOVA analysis (Haseman et al. 2001). Thus, regression analyses were also employed to evaluate the *subtle mechanistic effects* of GNPs on hormone accumulation in culture as a function of target-gene expression. All statistical analyses were conducted using SigmaPlot® 11 (Systat Software, Inc., Chicago, IL, USA) with $p<0.05$ considered to be statistically significant.

RESULTS

Characterization of Gold Nanoparticles

In the orientation viewed, HRTEM showed that the stock GNPs were faceted with a dominant interplanar distance of 0.232 (0.12) nm (mean [SD]; n= 40 measurements, N= 12 nanoparticles), which is congruent with face-centered-cubic gold {111} planes (Larios-Rodriguez et al., 2011) (Figure 2A). The MPD measured by HRTEM (6.58 [1.04] nm; Mean [SD])) was identical to that of our TEM (6.77 [1.25] nm Figure 2C) and SEM (7.63 [1.30] nm; Figure 2B) results. The weighted MPD of our stock GNPs, yielded from all EM observations, was 6.81 (1.25) nm (diameter range= 3.68 – 10.69 nm; n= 303 particles). TEM revealed little agglomeration (Figure 2C); however, SEM indicated that agglomerates were present in our stock solution (Figure 2B). A size-distribution analysis of the TEM results revealed that the majority of the stock GNPs were 5.0–7.0 nm in diameter (Figure 2D). DLS results confirmed the presence of agglomerates in our stock GNP solution (MHD = 243.7 [122.8] nm), which had a zeta potential of −24.4 (2.16) mV at pH 7.0 (Table S2).

TEM also showed that the MPD of the experimental GNPs was consistently ~10 nm regardless of particle concentration or time (Table S3). The vast majority (73.2%) of the experimental GNPs measured were ≤10 nm in diameter; however, some aggregation was present (Figure 2E). DLS revealed that the MHD of the experimental GNPs was consistently ~37.0 nm regardless of particle concentration (Table S2) or time (data not shown). The MHD within each GNP-containing culture medium was identical to that of culture medium without GNPs, suggesting that the high abundance of protein (~36.0 μg/mL) present in our samples was most likely masking detection of GNPs in each sample. The mean zeta potential of the culture medium was consistently ~ 9.0 mV, regardless of whether or not GNPs were present (Table S2).

XPS showed concomitant presence of molecular O_2, C, Na, Cl, Si, and K within the top few monolayers of the GNP surface (Table S4). The presence of O_2, C, and Na is indicative of residual sodium citrate from GNP synthesis (Kimling et al., 2006). Endotoxin assay results indicated that the overall mean concentration of endotoxin in pooled samples of supplemented culture medium, regardless of GNP concentration, was approximately 1.0 ng/mL (Table S5). Qualitative analysis revealed that endotoxin concentrations were variable (range = 0.476–2.24 ng/mL) among samples. The addition of GNPs to our culture solution did not significantly alter the relative concentration of endotoxin compared to culture medium alone (Table S5). The concentration of endotoxin did not increase as the concentration of GNPs decreased, suggesting that the GNPs present in each sample did not interfere with the Pyrogene™ assays.

Assessment of Gold Nanoparticles as Novel Endocrine Modulators

We estimated from the ISDD results that ~ 1.78×10^7, ~2.50×10^7, or ~3.28×10^7 GNPs were delivered to rat ovary upon exposure to 1.43×10^9 particles mL for 12, 24, or 48 hours, respectively (Table 1). Therefore, exposure of rat ovary to 1.43×10^6 particlesmL for 12, 24, or 48 hours in culture would theoretically yield target-tissue doses of ~ 1.78×10^5, ~2.50×10^5, and 3.28×10^5 GNPs, respectively (Table 1). Computer simulations indicated that gravity was not a significant factor in our model, confirming that the GNPs in culture diffused equally in all directions. This information was critical in validating our organ-culture model. Surprisingly, it was estimated that a mere 33 GNPs would be delivered to a rat ovary upon exposure to 1.43×10^3 particles mL for 48 hours (Table 1).

RIA was employed to evaluate the effects of GNPs on E2, P4, and inhibin secretion/accumulation *ex vivo*. Two-way ANOVAs showed no significant differences ($p>0.05$) in E2, P4, or inhibin secretion/accumulation in culture, compared to control, either as a function of GNP concentration or incubation period ($p>0.05$; Figure 3). Importantly, the accumulation of P4, E2, and inhibin from control ovaries did not decrease as a function of time, indicating that our experimental paradigm maintained ovarian viability (Figures S1). MRG-qPCR was used to assess effects of GNPs on ovarian steroidogenic and oxidative stress-related genes. This molecular approach was chosen to minimize the inherent biologic and technical variability in our qPCR data and monitor the inter-individual stability of reference gene expression in response to GNPs. We isolated approximately 40 ng RNA (260/280 nm = 1.85 ± 0.0052 and 260/230 nm = 2.31 ± 0.0095 [*mean + SEM*]) per rat ovary (n= 196). Two distinct bands of RNA were evident upon evaluation of RNA quality by gel electrophoresis (data not shown). Pearson correlation showed a significant positive relationship between the amount of total RNA isolated from control ovaries and the total RNA isolated from contralateral GNP-treated ovaries, suggesting that GNP-treatment had no effect on the integrity of ovarian RNA (Figure S2). Additionally, individual regression analyses showed no significant differences in RNA yield (ratio of total RNA from treated ovary/control ovary) as a function of either time (day of isolation) or animal trial (Figure S3). Gel electrophoresis and melting-curve analysis indicated the presence of a single gene product of expected size for each set of primers for each reference or target gene (data not shown). Qualitative evaluation of reference gene stability in response to GNPs yielded distinct variation in expression (Figure S4). Furthermore, the inter-animal (n=96 rats) coefficients of variation for *Z3h15, Gapdh*, and *Actb* in response to GNPs in our experimental paradigm were 4.64%, 5.96%, and 6.66%, respectively. Two-way ANOVA showed no significant differences in the relative expression of each individual target gene (*Star, Cyp11a1, Cyp17a1, Hsd3b1, Cyp19a1, Hmox1, or Sod2*) as a function of either time or GNP concentration ($p>0.05$, data not shown). However, linear regression analyses revealed a positive relationship between E2 accumulation and either *Cyp11a1* or *Star* expression, independent of time or GNP concentration (Figure 4A–B). Simple linear regression analyses indicated that E2 accumulation was positively associated with *Hsd3b1* and *Cyp17a1* expression, independent of incubation period or GNP concentration (Figure 4C–D). No significant relationship between either P4 or E2 accumulation and the relative expression of our other target genes was observed (Tables S5 and S6).

Extensive multiple-regression analyses were conducted to evaluate the subtle mechanistic relationships between either E2 or P4 accumulation and target gene expression, incubation period (time), and particle concentration (Tables S7–S9). Multiple-regression analyses showed that E2 accumulation was positively related to (a) *Cyp17a1* expression with time and particle concentration considered ($p<0.05$, adj $r^2= 0.080$); (b) *Hsd3b1* expression with time and concentration considered ($p<0.05$, adj $r^2= 0.096$); (c) both *Hsd3b1* and *Cyp17a1* expression independent of time or concentration ($p<0.001$, adj $r^2= 0.199$); and (d) both *Hsd3b1* and *Cyp17a1* expression with consideration of time and concentration ($p< 0.01$, $r^2= 0.234$, adj $r^2= 0.187$; Table S8). The relative expression of *Hsd3b1* or *Cyp17a1* partially accounted for the ability to predict E2 accumulation in these multiple-regression models—but was not related to particle concentration or incubation period. With regard to P4 accumulation, multiple-regression analyses revealed this endpoint to be associated with (a) *Star* expression with both time and particle concentration considered ($p<0.05$, adj $r^2= 0.064$); (b) *Star* expression with *Cyp11a1* expression considered independent of time or concentration ($p<0.01$, $r^2= 0.124$, adj $r^2= 0.102$); and (c) *Star* expression with *Cyp11a1* expression, time, and concentration considered ($p< 0.05$, adj $r^2= 0.0818$; Table S9).

The relative expression of *Star* was found to be the sole variable that partially accounted for the ability to predict P4 accumulation in all conducted multiple-regression analyses. In summary, extensive multiple-regression analyses revealed that the relative expression of *Hsd3b1* and *Cyp17a1* was the best predictor of E2 accumulation, and the relative expression of *Star* was shown to be the best predictor of P4.

Subsequent simple linear regression models were used to determine the concentration of GNPs responsible for the statistically significant positive relationships between hormone accumulation and target gene expression observed for each linear regression model in which pooled data were analyzed. These analyses indicated a positive relationship between either *Star* or *Cyp11a1* expression and P4 accumulation upon exposure to 1.43×10^6 particles/mL, regardless of incubation period (Figure 5A–B). Additional analyses showed significant positive relationships between E2 accumulation and relative expression of *Hsd3b1* or *Cyp17a1*, independent of time; upon exposure to 1.43×10^3 and 1.43×10^9 particles/mL, respectively (Figure 5C–D). Additional multiple-regression analyses that included time as a potential contributing factor confirmed the positive relationships derived from the simple linear regression models (Tables S10). However, further analyses showed that P4 accumulation was related solely to *Cyp11a1* expression despite concurrent consideration of *Star* expression and time ($p<0.01$, $r^2= 0.449$, adj $r^2= 0.386$; Table S11). A summary of all the concentration-specific regression models are presented in Tables S10 and S11. To summarize, *Star and Cyp11a1* genes were both predictors of P4 accumulation upon exposure of rat ovary to 1.43×10^6 particles/mL. In addition, *Hsd3b1* and *Cyp17a1* were found to partially predict E2 accumulation upon exposure of rat ovary to 1.43×10^3 or 1.43×10^9 particles/mL, respectively.

DISCUSSION

This is the first study to report that acute exposure of rat ovary to GNPs at low concentrations (*i.e.*, several orders of magnitude lower than those found in similar studies

[and Murphy 2010; Khlebtsov and Dykman 2011]) can subtly modulate the ovarian steroidogenic pathway *ex vivo*—independent of oxidative stress and inhibin (the latter is an important local mediator of ovarian steroidogenesis [Young and McNeilly 2012; Ho et al. 2006]). To illustrate, our lowest effective exposure dose (*i.e*. 1.43×10^3 particles/mL [equivalent to 8.07 pM AU or 0.00159]) is two- to three-fold less than the two lowest *in-vitro* exposure doses of GNPs (*i.e*., 20 and 27.0 pM) reviewed by Alkilany and Murphy (2010) and Khlebtsov and Dykman (2011). In addition, Phase-1 clinical studies of the anti-tumor compound CYT-6091 (a novel nanotherapeutic consisting of a ~30-nm GNP functionalized with molecules of tumor-necrosis factor alpha [TNF-α] and polyethylene glycol [PEG]) utilized a target dose of 1-mg TNF-α in a recent Phase-1 study (Libutti et al. 2010). Based on this reported Phase-1 dose and the ratio of gold (6.25 ppm) to TNF-α (250 ppb) in the calibrated dose of CYT-6091 described by Bischof et al. (2009), it can be estimated that approximately 350 ppb GNPs are administered with a dose of CYT-6091 that is calibrated to 1-mg TNF-α (assuming the average weight of Phase-1 participants to be 70 kg). That said, our lowest effective exposure dose of GNPs (*i.e.*, 0.00159 ppb) is approximately 220,000-fold less than the therapeutic dose of GNPs administered with CYT-6091. Even at our highest exposure dose, we remain within an order of magnitude of the targeted dose of CYT-6091. Hence, our results suggest that extremely low exposure doses, relative to realistic exposure conditions, of GNPs can modulate gene expression *ex vivo*.

Regression models revealed that *Star* and *Cyp11a1* expression was positively associated with P4 accumulation upon exposure to 1.43×10^6 particles/mL. Furthermore, E2 accumulation was positively associated with *Hsd3b1* and *Cyp17a1* expression upon exposure to 1.43×10^3 and 1.43×10^9 particles/mL, respectively. However, as evaluated by two-way ANOVA, our results showed no significant impact on summative gene expression or target-hormone accumulation in culture. Other research suggests a positive relationship between the expression of *Star, Cyplla1*, and *Cyp17a1* and the serum concentration of E2 in female mice chronically exposed to $Ti0_2$ nanoparticles (~6 nm, 10 mg/kg body weight) *in vivo* (Gao et al. 2012). However, chronic exposure of zebrafish to TiO_2 nanoparticles (240–280 nm, 0.1 mg/L) has been shown to significantly inhibit *Cyp11a1* expression (Wang et al. 2011). Hence, from a mechanistic standpoint, each target-tissue dose of GNPs might stimulate differential gene-regulatory pathways of our steroidogenic target genes, but increased exposure periods and/or GNP concentrations may be necessary to yield dramatic ovarian dysfunction. Collectively, this evidence points to *Star, Cyp11a1, Cyp17a1, Hsd3b1* as novel molecular targets of nanoparticle action that necessitate further research. Conversely, other studies have shown that ZnO (20–30 nm; Esmaeillou et al. 2013) and $Ca_3(PO4)_2$ (20–100 nm; Lui et al. 2010) nanoparticles had no effect on steroidogenesis *in vivo* or *in vitro*, respectively. These discrepant responses of ovarian steroidogenesis to nanoparticle exposure reported in the literature are conceivably mediated by the size, shape, composition, surface chemistry, and/or solubility of the nanoparticle being studied as well as the type of experimental model employed. These factors may contribute synergistically to the biophysicochemical characteristics of GNPs that coordinate specific nanoparticle-biologic interactions (*e.g*., formation of a nanoparticle-specific protein corona), which differ

from those of ZnO and/or $Ca_3(PO4)_2$ nanoparticles, that ultimately mediate the extent of observed nanotoxicity (Monopoli et al. 2012; Nel et al. 2009).

Our experimental approach entailing a paired ovarian-culture model was designed because it permitted (1) the examination of the inter-individual differences in ovarian sex-steroid output and gene expression; (2) the theoretical estimation of target-tissue dose using ISDD; and (3) the intraovarian architecture to remain intact. Interestingly, our ISDD results suggested that a target-tissue dose range of only 18–33 GNP mediated a subtle, yet statistically significant, stimulation of the steroidogenic pathway in the ovaries. To our knowledge, this is the lowest reported dose of GNPs shown to mediate a biologic response. However, it is critical that the limitations of the ISDD computational model be considered in the interpretation of these data.

ISSD estimates the number of particles that are delivered (*i.e.*, made available to the exposed tissue as a function of time) without a distinction made as to particle localization or thickness of ovary. It must also be taken into account that due to practical TEM considerations, the mean primary diameter (MPD) for input into the ISDD model (10 nm) entailed GNP concentrations that were 20-fold greater than those that we used experimentally. Therefore, the actual aggregation present in our cultures may have been less due to a decreased incidence of nanoparticle-nanoparticle interactions. Moreover, the experimental MPD, rather than the mean hydrodynamic diameter (MHD), was used for all ISDD computations because our DLS data suggested that the high protein content in our cultures inhibited detection of low-dose GNPs. The ratio of protein to GNPs in medium containing our highest exposure dose (1.59 ng/mL gold) was ~25:1, with the ratio increasing exponentially to ~25,000:1 and 250,000:1 for cultures containing medium- (1.59 pg/mL gold) and low-dose (1.59 fg/mL gold) GNPs, respectively. However, the presence of GNP-protein aggregates similar in size to those of single/aggregated proteins was also plausible. Hence, we alternatively use the MPD to *reasonably estimate* target-tissue dose. We postulated that the MPD increased from ~7.0 nm (stock GNPs) to ~10 nm (experimental GNPs) because the latter value takes into account the increased presence of aggregates observed after exposure to culture medium. Based on the parameters and limitations of the ISDD model, our dosimetric results demonstrated that low-dose GNPs were capable of modulating the ovarian steroidogenic pathway *ex vivo*, and as such, these data link target-tissue dose to a specific steroidogenic response.

The resultant r^2-values of our regression analyses indicated that the observed endocrine-modulating effects of GNPs resulted from a complicated multi-factorial subcellular mechanism that extends beyond transcriptional regulation of our chosen target genes. For instance, GNPs (4 and 13 nm) have been shown to transiently activate phase-I metabolizing enzymes (*e.g.*, CYP1A1 and CYP2B; Cho et al. 2010) and directly transfer electrons to CYP11A1 (Shumyantseva et al. 2005). Hence, we suggest that GNPs may enhance the enzymatic activity of CYP11A1, CYP17A1, and CYP19A1 since these enzymes exhibit biochemical similarities to those of CYP1A1 and CYP2B. Other evidence suggests that GNPs are capable of interacting with receptor-mediated signaling pathways (Tsai et al. 2012). Thus, we hypothesize that GNPs may also modulate estrogenic/progestogenic effects in rat ovary by interaction with steroid receptors via mechanisms that emulate those used by

other endocrine disruptors (Craig et al. 2011). It has been well established that low-dose exposures to endocrine disruptors (*e.g.*, TCDD and bisphenol A) modulate ovarian steroidogenesis via complex non-monotonic mechanisms (Vandenberg et al. 2012) that are distinct from those of linearly increasing exposures (Hutz et al. 2006). Additionally, we have shown that 10-nm GNPs enter and disrupt steroidogenic organelles of granulosa cells (Stelzer and Hutz 2009), increasing release of cholesterol precursor into the cytosol. The complex dynamics of *ex-vivo* particokinetics may also contribute to the overall variability observed.

Inter-individual differences among animals might also inherently contribute to the variability in our regression analyses. As shown with other toxicants (Miller 2001), inherent genetic variability could influence one's susceptibility to engineered nanomaterials that exhibit particular biophysicochemical properties. For this reason, we applied MRG-qPCR in order to control for such variability, and the present study is one of the first to do so in a nanotoxicologic study. MRG-qPCR is an advantageous molecular approach that has been shown to minimize inherent biologic and technical variation in qPCR data (Vandesompele et al. 2002). For example, Yin et al. (2010) have shown that the use of multiple reference genes prevented misleading qPCR results in a carbon-nanoparticle study. Thus, MRG-qPCR allowed us to monitor the inter-individual stability of reference gene expression so as to ensure that the observed changes in target-transcript abundance were due solely to GNP-exposure *ex vivo*. The adoption of MRG-qPCR to nanotoxicologic research is critical due to the unpredictability of nanoparticle-gene interactions and the complex intracellular behavior of GNPs *in situ*. The concentration of endotoxin (Esch et al. 2010) in our cultures was also evaluated to confirm that steroidogenic modulation was due to low-dose GNP exposure and not to this toxic confounder (Taylor and Terranova 1996). This evidence together with the lack of an oxidative-stress response in the present study suggests that the endotoxin present in our culture solutions did not contribute to the observed steroidogenic responses. Collectively, the reduced variability in reference gene expression afforded by MRG-qPCR and the endotoxin results increase our confidence that the steroidogenic responses observed in this study were indeed from exposure to low-dose GNPs.

CONCLUSIONS

The acute exposure of rat ovary to low-dose GNPs *ex vivo* subtly modulated the relationships between *Star* or *Cyp11a1* and progesterone accumulation as well as *Cyp17a1* or *Hsd3b1* and estradiol-17B accumulation, respectively. Thus, GNPs may represent a novel class of ovarian endocrine-modulating molecules that at elevated concentrations and/or durations of exposure could significantly perturb sex-steroid biosynthesis; which, in turn, could cause reproductive deficits in animals and humans. The data and mechanistic implications generated here (1) improve our understanding of genomic responses to GNPs by providing insight into the subcellular effects elicited on ovarian function; (2) serve as a foundation for future *in-vivo* studies of GNP-induced ovotoxicity in rat; and (3) from a public health standpoint, provide a molecular basis for potential female reproductive pathologies upon occupational or environmental exposure to GNPs.

Supplementary Material

Refer to Web version on PubMed Central for supplementary material.

ACKOWLEDGEMENTS

We offer thanks to Dr. Rebecca Klaper for allowing our use of the Malvern Zeta-sizer Nano Z, Dr. Qing Liu for his assistance with molecular techniques, and Dr. Devrah Arndt for acquisition of the SEM micrographs. We express sincere gratitude to Drs. Jugal Ghorai and Peter Dunn for their advice on statistical analyses. Thank you to Dr. Heather Owen for advice on imaging strategies. We thank Drs. Marija Gajdardziska-Josifovska, Marvin Schofield, and Donald Robertson for their collaborative acquisition of high-resolution TEM micrographs. We also thank Dr. Mark Engelhard of the Environmental Molecular Sciences Laboratory (EMSL) at Pacific Northwest National Laboratory, for characterizing our GNPs via x-ray photoelectron spectroscopy. This research was supported by the Children's Environmental Health Sciences Core Center at the University of Wisconsin – Milwaukee and Children's Research Institute (NIEHS P30 ES004184 PRJ32IR).

REFERENCES

Alkilany AM, Murphy CJ. Toxicity and cellular uptake of gold nanoparticles: what we have learned so far? J Nanopart Res. 2010; 12:2313–2333. [PubMed: 21170131]

Arnida, Janat-Amsbury MM, Ray A, Peterson CM, Ghandehari H. Geometry and surface characteristics of gold nanoparticles influence their biodistribution and uptake by macrophage. Eur J Pharm Biopharm. 2011; 77:417–423. [PubMed: 21093587]

Bischof JC, Goel R, Paciotti GF, Shah N, Visaria R. Biodistribution of TNF-[alpha]-coated gold nanoparticles in an in vivo model system. Nanomedicine. 2009; 4:401–410. [PubMed: 19505243]

Cai J, Jones DP. Superoxide in apoptosis: mitochondrial generation triggered by cytochrome c loss. J Biol Chem. 1998; 273:11401–11404. [PubMed: 9565547]

Chen YS, Hung YC, Lin LW, Liau I, Hong MY, Huang GS. Size-dependent impairment of cognition in mice caused by the injection of gold nanoparticles. Nanotechnology. 2010; 21(48):485102. [PubMed: 21051801]

Cho WS, Cho W, Jeong J, Choi M, Han BS, Shin Hs, Hong J, Chung BH, Jeong J, Cho MH. Size-dependent tissue kinetics of PEG-coated gold nanoparticles. Toxicol Appl Pharmacol. 2010; 245:116–123. [PubMed: 20193702]

Craig ZR, Wang W, Flaws JA. Endocrine-disrupting chemicals in ovarian function: effects on steroidogenesis, metabolism and nuclear receptor signaling. Reproduction. 2011; 142:633–646. [PubMed: 21862696]

Diemer T, Allen JA, Hales KH, Hales DB. Reactive oxygen disrupts mitochondria in MA-10 tumor leydig cells and inhibits steroidogenic acute regulatory (StAR) protein and steroidogenesis. Endocrinology. 2003; 144:2882S–2891S.

Esch RK, Han LI, Karin K, Foarde KK, Ensor SD. Endotoxin contamination of engineered nanomaterials. Nanotoxicology. 2010; 4:73–83. [PubMed: 20795903]

Esmaeillou M, Moharamnejad M, Hsankhani R, Tehrani AA, Maadi H. Toxicity of ZnO nanoparticles in healthy adult mice. Environ Toxicol Pharmacol. 2013; 35:67–71. [PubMed: 23262039]

Gao W, Xu K, Ji L, Tang B. Effect of gold nanoparticles on glutathione depletion-induced hydrogen peroxide generation and apoptosis in HL7702 cells. Toxicol Lett. 2011; 205:86–95. [PubMed: 21621595]

Gao G, Yuguan Z, Bing L, Zhao X, Zhang T, Sheng L, Hu R, Gui S, Sang X, Sun Q, Cheng J, Cheng Z, Wang L, Tang M, Hong F. Ovarian dysfunction and gene-expression characteristics of female mice caused by long-term exposure to titanium dioxide nanoparticles. J Hazard Mater. 2012; 243:19–27. [PubMed: 23131501]

Harper SL, Carriere JL, Miller JM, Hutchinson JE, Maddux BLS, Tanguay RL. Systemic evaluation of nanomaterials toxicity: utility of standardized materials and rapid assays. ACS Nano. 2011; 5:4688–4697. [PubMed: 21609003]

Haseman JK, Bailer AJ, Kodell RL, Morris R, Portier K. Statistical issues in the analysis of low-dose endocrine disruptor data. Toxicol Sci. 2001; 61:201–210. [PubMed: 11353128]

Hamada T, Watanabe G, Kokuho T, Taya K, Sasamoto S, Hasegawa Y, Miyamoto K, Igarashi M. Radioimmunoassay of inhibin in various mammals. J Endocrinol. 1989; 122:697–704. [PubMed: 2509617]

Hinderliter PM, Minard KR, Orr G, Chrisler WB, Thrall BD, Pounds JG, Teeguarden JG. ISDD: A computational model of particle sedimentation, diffusion and target cell dosimetry for in vitro toxicity studies. Part Fibre Toxicol. 2010; 7:36. [PubMed: 21118529]

Ho HM, Oshima K, Watanabe G, Taya K, Strawn EY, Hutz RJ. TCDD increases inhibin A production by human luteinized granulosa cells in vitro. J Reprod Dev. 2006; 52:523–528. [PubMed: 16627953]

Hussain S, Vanoirbeek JA, Luyts K, De Vooght V, Verbeken E, Thomassen LC, Martens JA, Dinsdale D, Boland S, Marano F, Nemery B, Hoet PH. Lung exposure to nanoparticles modulates an asthmatic response in a mouse model. Eur Respir. J. 2011; 37:299–309. [PubMed: 20530043]

Hutz RJ, Carvan MJ, Baldridge MG, Conley LK, Heiden TK. Environmental toxicants and effects on female reproductive function. Tren Reprod Bio. 2006; 2:1–11.

Kessler R. Engineered nanoparticles in consumer products. Environ Health Perspect. 2011; 119:a120–a125. [PubMed: 21356630]

Khlebtsov N, Dykman L. Biodistribution and toxicity of engineered gold nanoparticles: a review of in vitro and in vivo studies. Chem Soc Rev. 2011; 40:1647–1671. [PubMed: 21082078]

Kimling J, Maier M, Okenve B, Kotaidis V, Ballot H, Plech A. Turkevich method for gold nanoparticle synthesis revisited. J Phys Chem B. 2006; 110:15700–15777. [PubMed: 16898714]

Larios-Rodriguez E, Rangel-Ayon C, Castillo SJ, Zavala G, Herrera-Urbina R. Bio-synthesis of gold nanoparticles by human epithelial cells, in vivo. Nanotechnology. 2011; 22:355–601.

Li JJ, Lo SL, NG CT, Gurung RL, Hartono D, Hande MP, Ong CN, Bay BH, Yung LY. Genomic instability of gold nanoparticles treated human lung fibroblast cells. Biomaterials. 2011; 32:5515–5523. [PubMed: 21543115]

Libutti SK, Paciotti GF, Byrnes AA, Alexander HR Jr, Gannon WE, Walker M, Sqidel GD, Yuldasheva N, Tamakarin L. Phase 1 and pharmacokinetic studies of CYT-6091, a novel PEGlyated colloidal gold-rhTNF nanomedicine. Clin Cancer Res. 2010; 16:6139–6149. [PubMed: 20876255]

Lui X, Qin D, Cui Y, Chen L, Li H, Chen Z, Gao L, Li Y, Liu J. The effect of calcium phosphate nanoparticles on hormone production and apoptosis in human granulosa cells. Reprod Biol Endocrinol. 2010; 8:32. [PubMed: 20359372]

Miller MC III, Mohrenweiser HW, Bell DA. Genetic variability in susceptibility and response to toxicants. Toxicol Lett. 2001; 120:269–280. [PubMed: 11323185]

Monopoli MP, Aberg C, Salvati A, Dawson A. Biomolecular coronas provide the biological identity of nanosized materials. Nat Nanotechnol. 2012; 7:779–786. [PubMed: 23212421]

Nel AE, Mädler L, Velegol D, Xia T, Hoek EM, Somasundaran P, Klaessig F, Castranova V, Thompson M. Understanding biophysicochemical interactions at the nano-bio interface. Nat Mater. 2009; 8

Ngo YH, Li D, Simon GP, Garnier G. Paper surfacs functionalized by nanoparticles. Adv Colloid Interface Sci. 2011; 163:23–38. [PubMed: 21324427]

Pfaffl MW. A new mathematical model for relative quantification in real-time RT-PCR. Nucleic Acids Res. 2001; 29:e45. [PubMed: 11328886]

Shumyantseva VV, Carrara S, Bavastrello V, Riley JD, Skryabin KG, Archakov AI, Nicolini C. Direct electron transfer between cytochrome P450scc and gold nanoparticles on screen-printed rhodium-graphite electrodes. Biosens Bioelectron. 2005; 21:217–222. [PubMed: 15967373]

Stelzer RV, Hutz RJ. Gold nanoparticles enter rat ovarian granulosa cells and subcellular organelles, and alter *in-vitro* estrogen accumulation. J Reprod Develop. 2009; 55:685–690.

Sung JH, Ji JH, Park JD, Song MY, Song KS, Hyeon RR, Yoon JU, Jeon KS, Jeong J, Han BS, Chung YH, Chang HK, Lee JH, Kim DW, Kelman BJ, Yu IJ. Subchronic inhalation toxicity of gold nanoparticles. Part Fibre Toxicol. 2011; 8:16. [PubMed: 21569586]

Taylor CC, Terranova PF. Lipopolysaccharide inhibits in vitro luteinizing hormone-stimulated rat ovarian granulosa cell estradiol but not progesterone secretion. Biol Reprod. 1996; 54:1390–1396. [PubMed: 8724369]

Trkulja V, Lackovic Z. Vagal Influence on compensatory ovarian growth is important only briefly after hemicastration. Exp Biol Med. 2001; 226:776–781.

Truong L, Tilton SC, Zaikova T, Richman E, Waters KM, Hutchinson JE, Tanguay RL. Surface functionalities of gold nanoparticles impact embryonic gene expression responses. Nanotoxicology Early Online. 2012:1–10.

Tsai CY, Lu SL, Hu CW, Yeh CS, Lee GB, Lei HY. Size-dependent attenuation of TLR9 signaling by gold nanoparticles in macrophages. J Immunol. 2012; 188:68–76. [PubMed: 22156340]

Vandenberg LN, Colborn T, Hayes TB, Heindel JJ, Jacobs DR Jr, Lee D-H, Shioda T, Soto AM, vom Saal FS, Welshons WV, Zoeller RT, Myers JP. Hormones and endocrine-disrupting chemicals: low-dose effects and nonmonotonic dose responses. Endocr Rev. 2012; 33:378–455. [PubMed: 22419778]

Vandesompele J, De Preter K, Pattyn F, Poppe B, Van Roy N, De Paepe A, Speleman. Accurate normalization of real-time quantitative RT-PCR data by geometric averaging of multiple control genes. Genome Biol. 2002; 3 research0034.1-0034.11.

Wang J, Zhu X, Zhang X, Zhao Z, Liu H, George R, Wilson-Rawls J, Chang Y, Chen Y. Disruption of zebrafish (Danio rerio) reproduction upon chronic exposure to TiO2 nanoparticles. Chemosphere. 2011; 83:461–467. [PubMed: 21239038]

Woodrow Wilson International Center for Scholars: A nanotechnology consumer products inventory. Available at: http://www.nanotechproject.org/consumerproducts.

Yin R, Tian F, Frankenberger B, de Angelis MH, Stoeger T. Selection and evaluation of stable housekeeping genes for gene expression normalization in carbon nanoparticle-induced acute pulmonary inflammation in mice. Biochem Biophys Res Commun. 2010; 399:531–536. [PubMed: 20678479]

Young JM, McNeilly AS. Inhibin removes the inhibitory effects of activin on steroid enzyme expression and androgen production by normal ovarian thecal cells. J Mol Endocrinol. 2012; 48:49–60. [PubMed: 22082494]

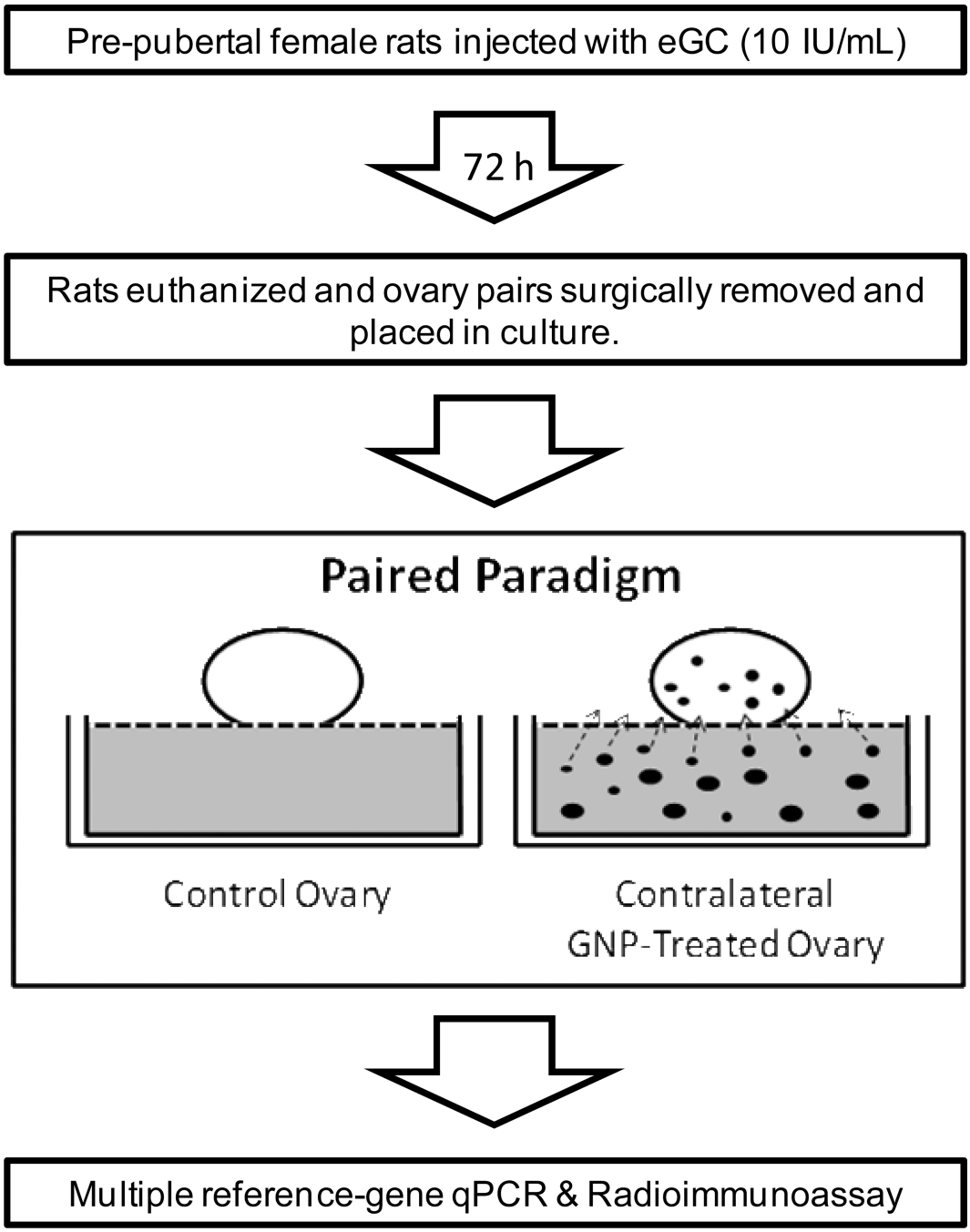

Figure 1.
Simplified schematic representation of the paired *ex-vivo* paradigm employed to evaluate potential endocrine-modulating effects of GNPs on rat ovaries in culture.

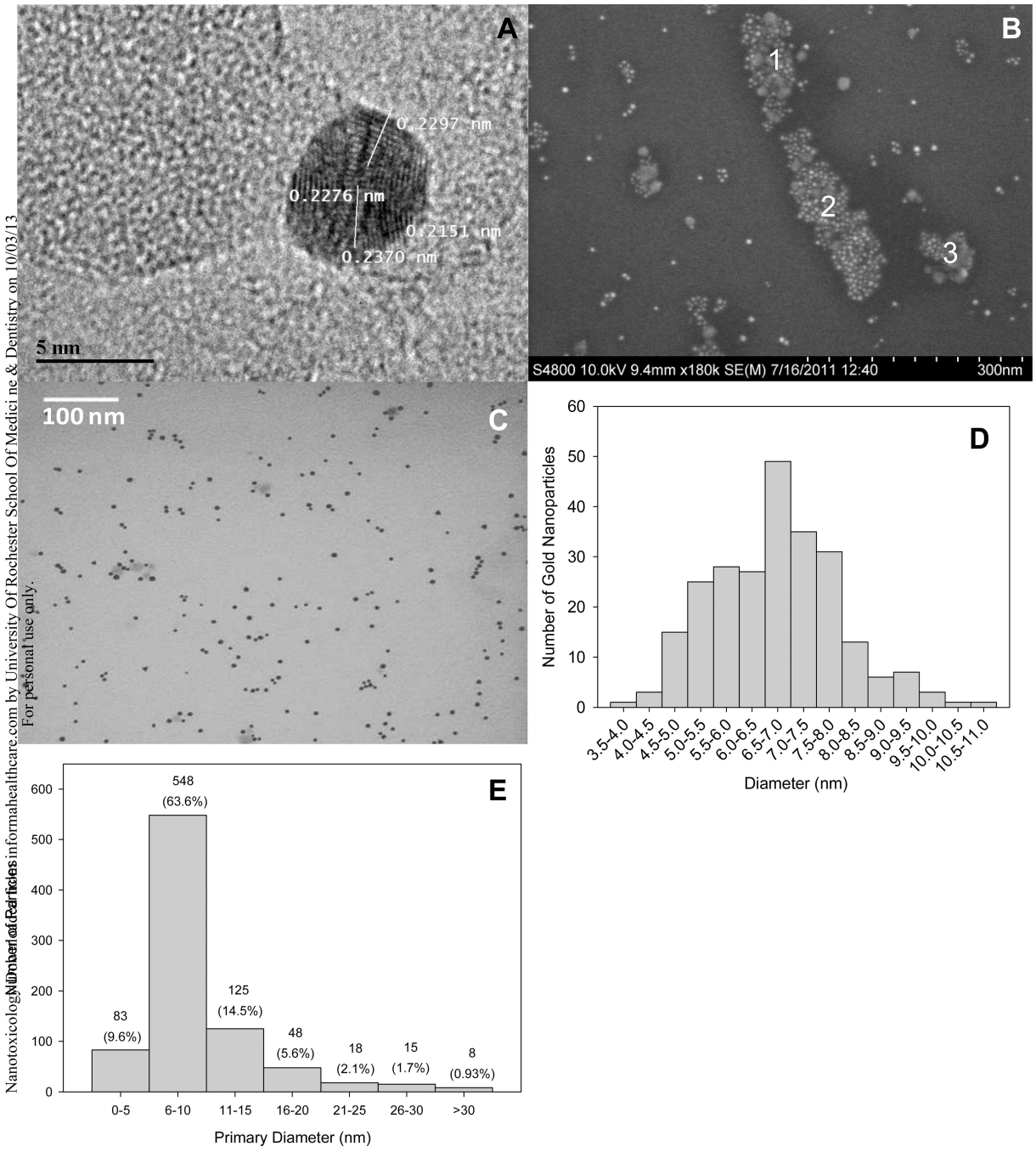

Figure 2.

(A) HRTEM photomicrograph of stock gold nanoparticles on a carbon- and formvar-coated copper grid. (B) SEM photomicrograph of stock gold nanoparticles in double-distilled water. Aggregates of diverse size and morphology were present. The size dimensions of aggregates *1–3* were measured to be 155.7×64.3 nm (length × width), 249.7×65.1 nm, and 75.0 × 51.2 nm, respectively. (C) TEM photomicrograph of stock gold nanoparticles in double-distilled water. (D) Size distribution of stock GNPs as measured by TEM. The number of GNPs within designated size cohorts is presented. (E) Size distribution of GNPs (n= 861), as

evaluated by TEM, upon exposure to the conditions of our *ex-vivo* paradigm. Data were pooled independent of particle concentration and incubation period.

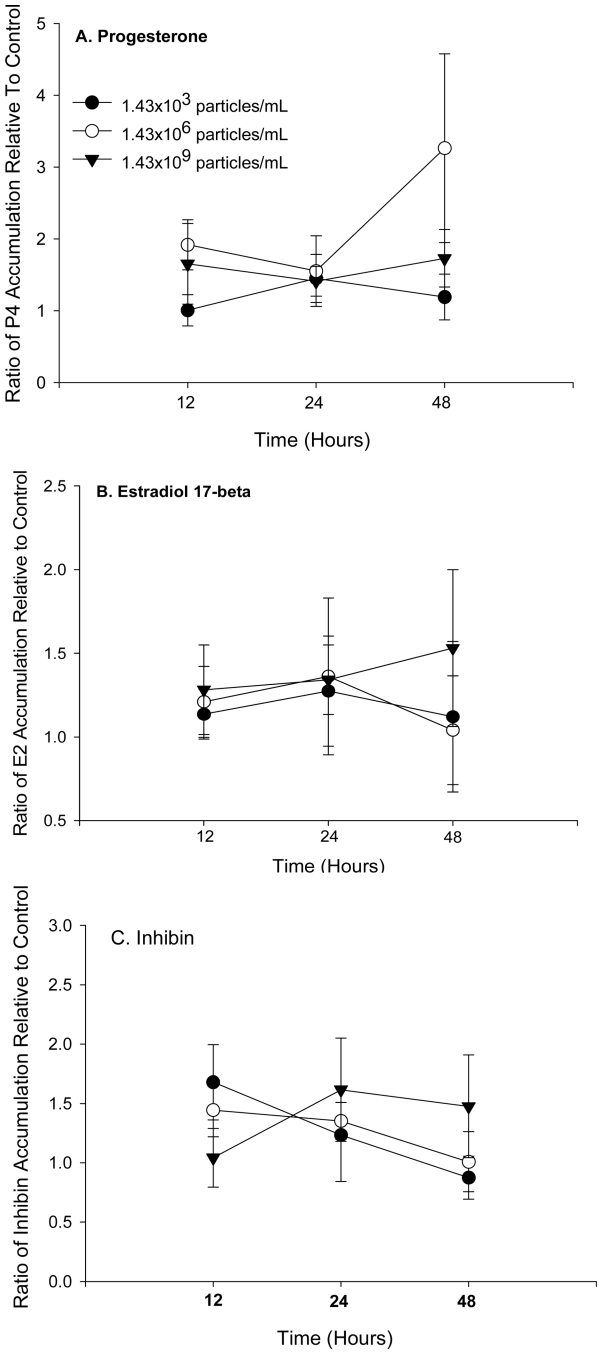

Figure 3.

Two-way ANOVAs showed no significant differences in either (A) progesterone (df= 82, $p>0.05$), (B) estradiol-17β (df= 69 ovaries, $p>0.05$), or inhibin (df= 76, $p>0.05$) secretion/accumulation *ex vivo*, compared to control, either as a function of GNP concentration or of incubation period.

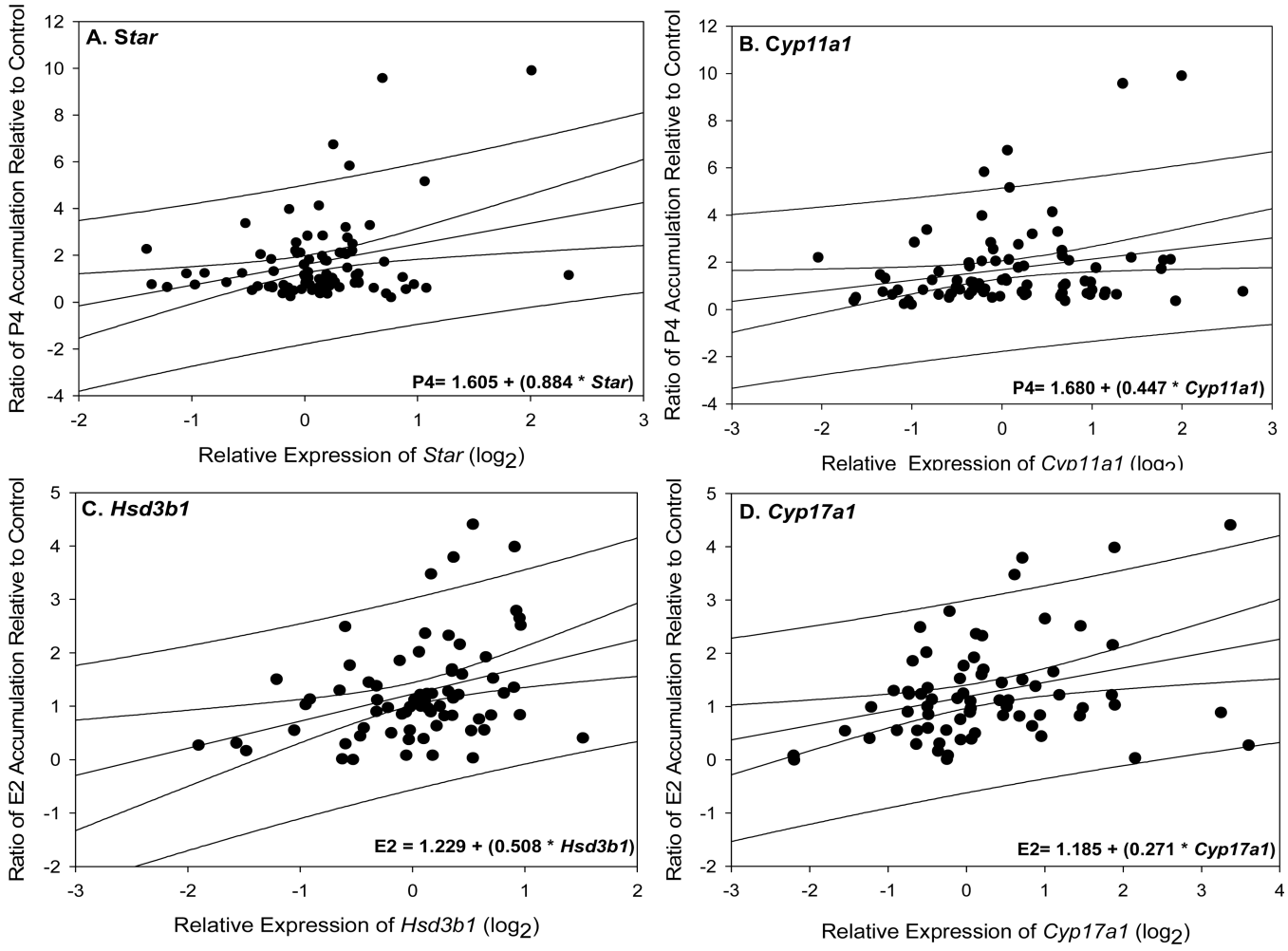

Figure 4.

(**A**–**B**) Effect of GNPs on ovarian progesterone (P4) and *Star* or *Cyp11a1* expression. Regression analyses indicated that positive relationships existed between *ex-vivo* accumulations of P4 and the relative expression of (**A**) *Star* (df= 82 rats, p= 0.006, r^2= 0.0891, adj r^2= 0.0779) or (**B**) *Cyp11a1* (df= 82, p= 0.032, r^2= 0.0554, adj r^2= 0.0437),) upon exposure to GNPs. (**C**–**D**) Effect of GNPs on estradiol 17-β (E2) and *Hsd3b1* or *Cyp17a1* expression. Regression analyses indicated that positive relationships existed between *ex-vivo* accumulations of E2 and the relative expression of (**C**) *Hsd3b1* (df= 69 rats, p= 0.003, r^2= 0.120, adj r^2= 0.107) or (**D**) *Cy17a1* (df= 69 rats, p= 0.006, r^2= 0.1059, adj r^2= 0.0922) upon exposure to GNPs. Data were pooled prior to statistical analysis; thus, factors of time and concentration were not considered.

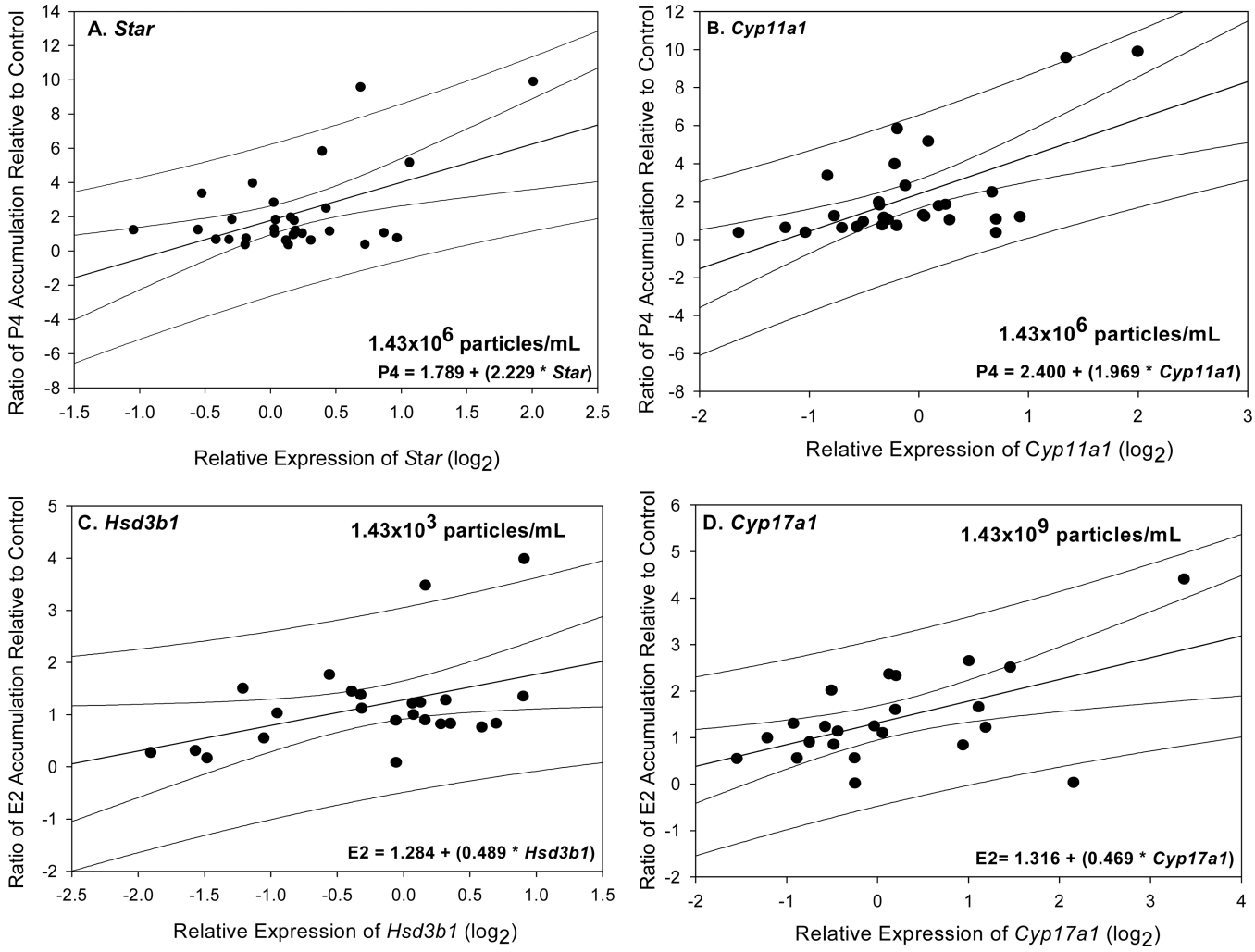

Figure 5.

(**A–B**) Concentration-specific effect of GNPs on ovarian progesterone (P4) and *Star* or *Cyp11a1* expression. Linear regression models showed that P4 accumulation was positively associated with both (**A**) *Star* (n=30 rats, p= 0.003, r^2= 0.278, adj. r^2= 0.252) and (**B**) *Cyp11a1* (n=30 rats, p<0.001, r^2= 0.366, adj r^2= 0.344) expression upon exposure of rat ovaries to 1.43×10^6 particles/mL, independent of time. (C-D) Concentration-specific effects of GNPs on estradiol 17-β (E2) and *Hsd3b1* or *Cyp17a1* expression. Linear regression models revealed significant positive relationships between E2 accumulation and the expression of either (**C**) *Hsd3b1* (n=24 rats, p= 0.038, r^2= 0.181, adj r^2= 0.144) or (**D**) *Cyp17a1* (n=23 rats, p= 0.007, r^2= 0.301, adj r^2= 0.0.268) in response to 1.43×10^3 or 1.43×10^9 particles/mL, respectively. Data were pooled for each specified concentration, independent of incubation period. The administered dose (particles/mL; *top right*) and regression equation (*bottom right*) associated with each respective analysis are presented.

Table 1

Summary of the target doses of GNPS delivered to rat ovaries *ex vivo* as estimated using the ISDD computational model.

Exposure (particles/mL)	Time (h)	Fraction (%)	Mass (μg)	Surface area (cm^2)	Particle Number
1.43×10^3	12	1.13×10^{-5}	1.80×10^{-10}	1.51×10^{-11}	18
	24	1.59×10^{-5}	2.52×10^{-10}	2.13×10^{-11}	25
	48	2.09×10^{-5}	3.32×10^{-10}	3.00×10^{-11}	33
1.43×10^6	12	1.13×10^{-2}	1.80×10^{-7}	1.51×10^{-8}	17,850
	24	1.59×10^{-2}	2.52×10^{-7}	2.13×10^{-8}	24,951
	48	2.09×10^{-2}	3.32×10^{-7}	3.00×10^{-8}	32,834
1.43×10^9	12	11.34	1.80×10^{-4}	1.51×10^{-5}	17,849,895
	24	15.86	2.52 × 10-4	2.13 × 10-5	24,950,959
	48	20.87	3.32×10^{-4}	3.00×10^{-5}	32,834,179

Each fraction delivered is presented as the estimated percentage of each respective administered dose of GNPs that is delivered to each rat ovary as a function of incubation period (time) and particle concentration. Computational results were normalized to account for the fact that the surface area of the ovary was approximately 25% that of the 1-mL center well dish. Estimated target doses are presented on the basis of total mass, surface area, and particle number delivered.